

Development of a high stability L-band radiometer for ocean salinity measurements

Alan B Tanner, William J Wilson

Jet Propulsion Laboratory,
California Institute of Technology
Pasadena, California USA
alan.b.tanner@jpl.nasa.gov

Fernando A Pellerano

Goddard Space Flight Center
Greenbelt, Maryland USA

Abstract—An NEDT analysis of a Dicke radiometer with noise diode injection is presented. The analysis is formulated for a calibration that would form separate running averages of receiver noise temperature and of gain in order to minimize the NEDT and maximize the antenna observation duty cycle relative to the reference and noise diode duty cycles. Results are applied to the Aquarius ocean salinity radiometer problem to show that near ideal total-power radiometer performance is possible.

Keywords—microwave radiometer; noise equivalent delta-T; NEDT

I. INTRODUCTION

This talk will present some early results of a research effort being conducted jointly between NASA's Goddard Space Flight Center (GSFC) and the Jet Propulsion Laboratory (JPL) to develop a so called Ultra Stable microwave Radiometer (USR). This work is applicable to the Aquarius sea surface salinity mapping mission, the primary instrument of which will be an L-band (1.4 GHz) radiometer to measure the ocean emissivity from space. The performance required of this radiometer- due to the narrow range of signal over the ocean- is 0.1 K of brightness temperature uncertainty. At this level there are many design problems to solve before such requirements can be guaranteed.

Thus far our research has focused on thermal models of the radiometer electronics and on calibration schemes that will be needed to achieve the required noise-equivalent delta-T (NEDT). We have built a laboratory thermal testbed and radiometer breadboard, conducted tests, and used the data to test these schemes, assumptions, and system models. We have conducted thermal tests of radiometer components such as noise diodes, amplifiers, couplers, coaxial cable, and switches- all of which showed significant sensitivities in the range of 500 to 5000 parts per million per degree C (ppm/C). We have applied and compared these data to tests of the assembled radiometer system. These data have established some practical limits with which a radiometer can be stabilized in the presence of time variable thermal gradients. We have translated these results to temperature sensing and thermal stability requirements for Aquarius. We have also measured the gain and receiver noise temperature spectra and apply these data to a new calibration scheme which achieves near ideal NEDT performance by applying long running averages of the receiver noise temperature and of the receiver gain to the brightness

temperature estimate. Our talk will present many of our results. This paper, however, is limited to the mathematical details of our NEDT calculation.

II. THE NOISE EQUIVALENT DELTA-T (NEDT)

The NEDT of Aquarius needs to approach that of an ideal total power radiometer, given the available bandwidth and observation time, yet such performance is not necessarily attainable since the observation time must be divided between internal calibrators. Figure 1 illustrates the topology of a Dicke radiometer with noise injection, along with an example of the radiometer's output voltage versus time to illustrate the basic measurement sequence. The calibration circuits of this radiometer consists of the Dicke switch and noise diode. The Dicke switch alternates between the antenna and the reference load temperatures, T_A and T_o , and the noise diode adds a calibrated antenna-equivalent noise temperature, T_{ND} , to the received signal. As shown, the reference load and noise diodes are applied every τ seconds with duty cycles d_o and d_N , respectively, leaving a remainder of $1-d_o-d_N$ duty cycle to measure the antenna noise temperature. The noise diode is injected after the Dicke switch in Figure 1, so the noise diode response can be measured in either mode of the Dicke switch. For our calculations, however, we will assume that the noise diode is injected only while this switch is in the reference mode. The response of the radiometer to each source is integrated and recorded separately as C_o , C_N , and C_A , and all measurements are subject to the unknown and time variable quantities of receiver gain, G , and additive receiver noise temperature, T_r , as summarized in the figure.

In the simplest mode of operation the antenna temperature T_A can be estimated from each measurement cycle as

$$T_A = T_o - (C_o - C_A) \frac{T_{ND}}{C_N - C_o}, \quad (1)$$

where we see that G and T_r from the expressions of Figure 1 cancel. Equation (1) is inefficient from a noise standpoint since it makes no assumptions about the stability of the receiver gain or the receiver noise temperature other than that these factors are common to all of the measurements within the interval τ . If, on the other hand, we know that G or T_r are stable over longer time scales we can reformulate the calibration as follows: we estimate the antenna brightness temperature over the i 'th measurement interval according to

$$T_{Ai} = g_{mi} C_{Ai} - T_{mi}, \quad (2)$$

where g is the inverse of gain ($g=G^{-1}$), the i subscripts are time indices, and m and n denote running averages to be discussed below. C_{Ai} is a boxcar integration of the antenna response lasting τ_A seconds centered on time $t=t_0+i\tau_A$ (where t_0 is an arbitrary time origin). This interval (τ_A) is set by mission requirements ($\tau_A=12$ seconds for Aquarius) and may be greater than τ (the Dicke interval). The measurements of g_{mi} and T_{mi} are computed from running averages spanning τ_g and τ_r seconds, respectively, as shown in Figure 1, according to

$$g_{mi} = \frac{1}{2m+1} \sum_{j=i-m}^{i+m} \left(d_o \frac{T_{oj} + T_{mi}}{C_{oj}} + d_n \frac{T_{oj} + T_{ND} + T_{mi}}{C_{Nj}} \right) \frac{1}{d_o + d_n} \quad (3)$$

and

$$T_{mi} = \frac{1}{2n+1} \sum_{j=i-n}^{i+n} C_{oj} \frac{T_{ND}}{C_{Nj} - C_{oj}} - T_{oj}. \quad (4)$$

where reference load and noise diode responses, C_{oi} and C_{Ni} , are measured on the same time grid as C_{Ai} such that $\tau_g = (2m+1)\tau_A$ and $\tau_r = (2n+1)\tau_A$. If $n=m=0$ then (2), (3), and (4) reduce to (1). Otherwise, we are interested in the case of $n>m>0$. Equations (3) and (4) are arranged to exploit an observed characteristic of microwave radiometers, which is that the receiver noise temperature is often much more stable than the gain. To put this in precise terms, we have measured the spectra of gain and of receiver noise temperature from an existing Ka-band (22 GHz) Advanced Water Vapor Radiometer (AWVR) at JPL [1], and found that their spectra fit the following equations: the normalized gain spectra (i.e. scaled to unity gain) was

$$S_g(f) = a_g + b_g / f \quad (5)$$

with $a_g = 1.2 \times 10^{-8}$ (gain²/Hz), $b_g = 8.1 \times 10^{-10}$ (gain²/Hz), and the measured receiver noise spectra was

$$S_r(f) = a_r + b_r / f \quad (6)$$

with $a_r = 0.11$ (K²/Hz), $b_r = 2.7 \times 10^{-5}$ (K²/Hz). The average receiver noise temperature in this case was about 450 K. These spectra were derived from time series measurements using (3) and (4) (with $n=m=0$). The 'white' noise terms, a_r and a_g , are consistent with theoretical noise limits for (3) and (4) given the detection bandwidth of the AWVR (500 MHz), the calibration duty cycles ($d_n=0.15$ and $d_o=0.3$), and the magnitudes of T_r (450K), T_o (298K), and T_{ND} (300K). The $1/f$ terms, b_g and b_r , on the other hand, reflect the basic receiver stability, including the RF amplifiers and detector, and to some extent their thermal stability since the amplifiers are known to have a large temperature coefficient. To compare b_g and b_r we note that in the context of (3) we should normalize b_r by the system noise temperature; this yields $b_r/(450+298)^2 = 4.8 \times 10^{-11}$, which is about 17 times lower than b_g . Thus, we see that the receiver noise is more stable than the receiver gain. This phenomenon may be related to the fact that the system gain is subject to the stability of a chain of many transistors, whereas the noise figure depends only on the first transistor of the LNA. We should add to these observations that: 1) the AWVR have exceptionally good temperature control (which undoubtedly helps to keep the $1/f$ noise low); 2) the net RF gain is about 90 dB (this is a direct-detect single sideband receiver); and 3) the transistors are all GaAs FETs.

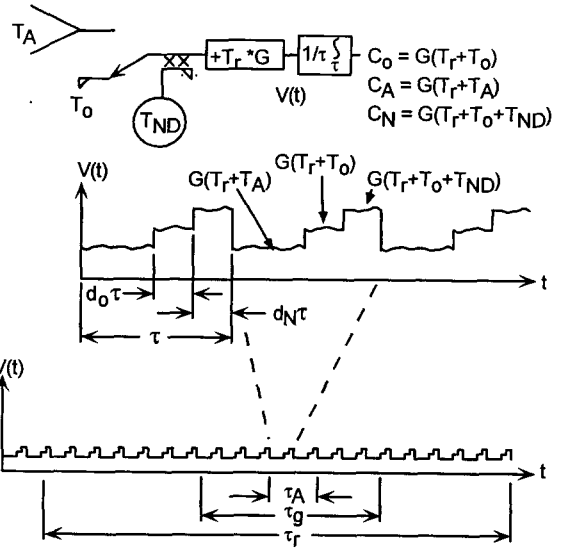


Figure 1. Radiometer and timing model

Equations (2) thru (6) are sufficient to derive an expression for the NEDT of the radiometer given the duty cycles and integration times of Figure 1. We start by evaluating the expected value of $(T_{roi} - T_{mi})^2$ in the presence of just the $1/f$ noise of (6) (i.e. set $a_r=0$). This represents the error between the short-term (τ_A) and long-term (τ_r) averages of the 'true' T_r . This error is zero at $\tau_r = \tau_A$, and increases for $\tau_r > \tau_A$. Janssen [2] provides the needed autocorrelation function of boxcar averaged $1/f$ noise processes for this calculation. Next, we evaluate the white-noise variance of T_{mi} from a_r of (6). This represents the error in the estimate of T_r which decreases as τ_r increases. Adding these results yields the net variance in the T_r estimation error:

$$\sigma_{T_r}^2 = \frac{a_r}{2\tau_A} \left(\frac{1}{2n+1} + \frac{1}{2n+1} \right) + \frac{1}{2\tau_A} \left(\frac{1}{2n+1} \right) \left(\frac{2(n+1)^2}{2n+1} \ln(n+1) - \frac{2n^2}{2n+1} \ln(n) - \ln(2n+1) \right) \quad (7)$$

which for sufficiently small τ_A has a minimum at

$$\tau_r = (2n+1)\tau_A = \frac{a_r}{2b_r}. \quad (8)$$

Similar equations apply to the gain estimation error, given (5).

Next, we expand each of the terms in (2) into their expected values and an explicit normalized measurement error as follows:

$$T_{Ai} = \langle T_{Ai} \rangle + (1+\delta_{Ti}) = \langle g_{mi} \rangle + (1+\delta_{gmi}) \langle C_{Ai} \rangle + (1+\delta_{Ai}) - \langle T_{mi} \rangle + (1+\delta_{mi}) \quad (9)$$

where $\langle \rangle$ is the expectation operator and each δ term is a zero-mean normalized random variable which represents the fractional error of each measurement. This approach, in which we replace every random variable X with δ_X using $X = \langle X \rangle + \delta_X$, simplifies the algebra which follows. For example, δ_{gmi} and δ_{Ai} are both much smaller than 1, in which case $(1+\delta_{gmi})(1+\delta_{Ai}) \approx 1 + \delta_{gmi} + \delta_{Ai}$. With this and with the identity $\langle T_{Ai} \rangle = \langle g_{mi} \rangle \langle C_{Ai} \rangle - \langle T_{mi} \rangle$, (9) becomes

$$T_A \delta_{Ti} \approx (T_A + T_r)(\delta_{gmi} + \delta_{Ai}) - T_r \delta_{mi}. \quad (10)$$

Here, we have also dropped the “i” indices and expectation operator notations with the understanding that $T_r = \langle T_{ri} \rangle$, etc.. The left side of (10) is the brightness temperature estimation error, the standard deviation of which is the NEDT that we seek. The remaining task is to evaluate the variance of δ_{Ti} by expanding the errors on the right side of (10) into independent error terms. The first term, δ_{Ai} , needs no further expansion since this is the white noise associated with the antenna measurement C_{Ai} , which is uncorrelated with the other errors. The variance of δ_{Ai} is readily calculated as $\langle \delta_{Ai}^2 \rangle = [B(1-d_N-d_o)\tau_A]^{-1}$, where B is the detection bandwidth and the other terms are from Figure 1. The δ_{gmi} and δ_{mi} terms, however, are partially correlated since both involve white noise from C_{oj} and C_{Nj} and 1/f errors of T_{mi} . To evaluate these errors we separate δ_{gmi} and δ_{mi} into their constituent 1/f and white noise terms, and then use (3) and (4) to further expand the white noise errors in terms of the errors associated with C_{oj} and C_{Nj} . From (4) the normalized receiver noise error expands to

$$\delta_{mi} \cong \delta_{mif} + \frac{(T_{ND} + T_o + T_r)(T_o + T_r)}{T_r T_{ND}} (\delta_{oni} - \delta_{Nni}) \quad (11)$$

where δ_{mif} is the 1/f error and δ_{oni} and δ_{Nni} are the white noise errors associated with the averages of C_{oj} and C_{Nj} in (4) (i.e. after averaging $2n+1$ samples), respectively. Equation (11) is an approximation since the identity $(1+\delta)^{-1} \cong (1-\delta)$ has been used to bring δ_{Nni} out of the denominator. Likewise, from (3) the normalized gain error expands to

$$\delta_{gmi} \cong \delta_{gmif} + \frac{1}{d_o + d_N} \left[-d_o \delta_{omi} - d_N \delta_{Nmi} + \delta_{mmif} \left(\frac{d_o}{T_r + T_o} + \frac{d_N}{T_r + T_{ND} + T_o} \right) \right] \quad (12)$$

where δ_{gmif} is the gain 1/f error and δ_{omi} and δ_{Nmi} are the white noise errors associated with C_{oj} and C_{Nj} after computing the $2m+1$ sample average in (3). In (12) we have also added another subscript, m, to the receiver noise error, which now appears as δ_{mmi} to distinguish it from δ_{mi} of (11). These errors differ slightly because of the different integration times, τ_A and τ_g , which apply to the 1/f error of (7): note that the receiver noise 1/f instability will not contribute any error to the gain estimate if $\tau_g = \tau_r$, so we see that this error should be evaluated in (7) by replacing τ_A with τ_g . Otherwise, the white noise component of δ_{mmi} is identical to that of (11).

To form the final expression for the NEDT of the system we combine (11) and (12) in (10), expand each of the δ terms until we identify the dependent and independent errors, regroup the dependant errors, and then evaluate the variance of the final expression as the sum of variances of the independent terms. This leads to a very lengthy expression, which for the specific case of $\tau_g \ll \tau_r$ and $d_o = d_N$ can be approximated with the following:

$$T_A^2 < \delta_{Ti}^2 \rangle \cong (T_A + T_r)^2 \left[b_g \theta(m) + \frac{a_g}{2\tau_g} + \frac{1}{(1-2d_o)B\tau_A} \right] + \frac{1}{4} \left[b_r \theta \left(\frac{n-m}{2m} \right) + \frac{a_r}{2\tau_r} \right] \left[\frac{T_A + T_r}{T_r + T_o} + \frac{T_A + T_r}{T_r + T_{ND} + T_o} - 2 \right]^2 + b_r \theta \left(\frac{m-1}{2} \right) \quad (13)$$

where the function $\theta(x)$ was defined in (7), and

$$a_g = \frac{1}{Bd_o}, \text{ and } a_r = \frac{4}{Bd_o} \left[\frac{(T_{ND} + T_o + T_r)(T_o + T_r)}{T_{ND}} \right]^2 \quad (14)$$

Some sample NEDT calculations are presented in Table 1 using these analysis for a set of Aquarius system parameters, as summarized in the table. The b_g and b_r 1/f coefficients in this case have been measured in recent L-band breadboard tests as part of our ongoing developments, and differ slightly from those presented above from the AWVR. In the first row of Table 1 we have calculated optimized duty cycles which minimize the NEDT, and in subsequent rows we have applied constraints to those parameters which have been highlighted. In the first two rows the optimization calls for an extremely long τ_r , so we have constrained this parameter in subsequent rows with only a minor degradation in the NEDT. In alternate rows we have applied the constraint $d_o = d_N$ to show that the NEDT is insensitive to the reference versus noise diode duty cycles; only their sum is important. The last column indicated the performance relative to the ideal total power radiometer with $\Delta T = (T_A + T_R) / \sqrt{B\tau_A}$ ($=0.023$ K in this case).

TABLE I. NEDT OPTIMIZATION RESULTS

System parameters:					
$\tau_A = 12$ s					
$b_r = 6.5 \times 10^{-6}$ K ² /Hz					
$b_g = 2.0 \times 10^{-9}$ /Hz					
$T_r = 255$ K					
$T_o = 295$ K					
$T_{ND} = 500$ K					
$T_A = 100$ K					
$B = 20$ MHz					
τ_r (s)	a_r (s)	d_o	d_N	NEDT (K)	/TP
555630	96	0.24	0.02	.0375	1.64
157812	96	0.13	0.13	.0376	1.64
5000	86	0.19	0.10	.0381	1.66
5000	89	0.14	0.14	.0382	1.67
1000	71	0.23	0.12	.0401	1.75
1000	69	0.18	0.18	.0403	1.76

note: **highlighted** indicates constrained parameter

ACKNOWLEDGMENT

The work described was performed at the Jet Propulsion Laboratory, California Institute of Technology, under contract with the National Aeronautics and Space Administration.

REFERENCES

- [1] Tanner, A. B., and A. L. Riley, “Design and performance of a high-stability water vapor radiometer,” *Radio Sci.*, 38(3), 8050, doi:10.1029/2002RS002673, March 2003, <http://www.agu.org/pubs/crossref/2003/2002RS002673.shtml>
- [2] Janssen, M.A., et al., “Direct imaging of the CMB from space,” *ApJ*, 9602009, Feb. 1996, http://arxiv.org/PS_cache/astro-ph/pdf/9602/9602009.pdf